

A rate determining step change in the pre-steady state of acetylcholinesterase inhibitions by 1,*n*-alkane-di-*N*-butylcarbamates

Gialih Lin,* Hsin-Chang Tseng, Ai-Chi Chio, Tsao-Ming Tseng and Bo-Yi Tsai

Department of Chemistry, National Chung-Hsing University, Taichung, Taiwan

Received 21 October 2004; accepted 17 December 2004

Available online 19 January 2005

Abstract—Alkane-1-*N*-butylcarbamate-*n*-ols (**1–7**) and 1,*n*-alkane-di-*N*-butylcarbamates (**8–14**) are potent pseudo-substrate inhibitors of acetylcholinesterase. For inhibitors **1–7**, the pre-steady state $-\log K_s$ values and steady state $-\log K_i$ values are linearly correlated with the tether length (*N*). However, for inhibitors **8–14**, correlation of the $-\log K_s$ or $-\log K_i$ values against *N* deviates from linearity. A discontinuity of the $-\log K_s$ versus *N* plot, concave downwards, is indicative of a rate determining step change in the pre-steady state of acetylcholinesterase inhibitions by inhibitors **8–14**.

© 2004 Elsevier Ltd. All rights reserved.

The drugs used in Alzheimer's disease are cholinesterase inhibitors.¹ Two forms of cholinesterase coexist ubiquitously throughout the body, acetylcholinesterase (AChE, EC 3.1.1.7) and butyrylcholinesterase (BChE, EC 3.1.1.8), and although highly homologous, >65%, they are products of different genes on chromosomes 7 and 3 in humans, respectively.² The analogues of physo-

stigmine, an alkaloid extracted from a tropical plant, and rivastigmine (exelon) are all carbamate inhibitors and have been widely studied as potential drugs for Alzheimer's disease (Fig. 1).^{3–5} Carbamate inhibitors, such as rivastigmine and aryl carbamates, are characterized as 'pseudo-irreversible'⁵ or 'pseudo-pseudo-substrate'⁶ inhibitors of AChE (Scheme 1). Values of steady state

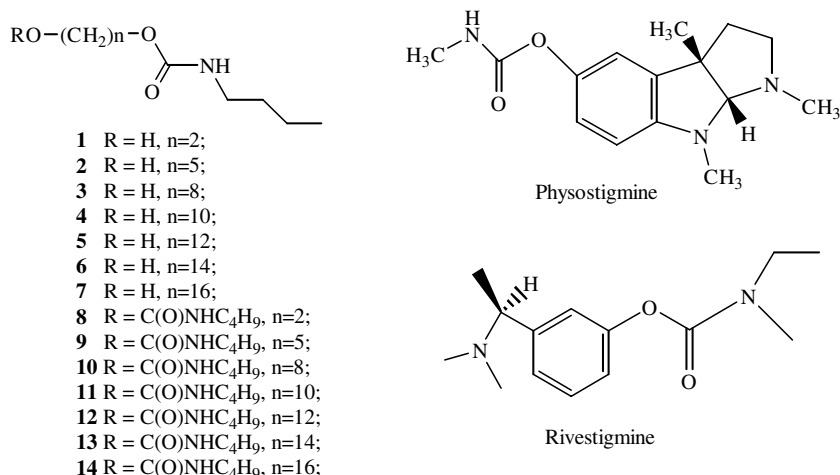
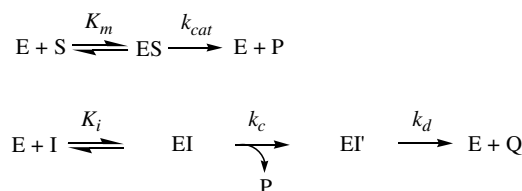
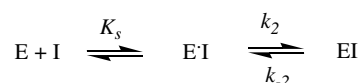


Figure 1. Chemical structures of tether inhibitors **1–14**, physostigmine, and rivastigmine.

* Corresponding author. Tel.: +886 4 2284 0411x705; fax: +886 4 2286 2547; e-mail: gilin@dragon.nchu.edu.tw



Scheme 1. Kinetic scheme for the steady state pseudo-substrate inhibitions of AChE in the presence of substrate. E, AChE enzyme; S, substrate; I, carbamate inhibitor; EI, the enzyme–carbamate inhibitor covalent tetrahedral intermediate; EI', the carbamyl enzyme intermediate; K_i , the dissociation constant of EI; k_c , carbamylation constant; P, the first product; k_d , decarbamylation constant; Q, the second product.



Scheme 2. Kinetic scheme for the pre-steady state AChE inhibitions. E, AChE enzyme; I, carbamate inhibitor; EI, the enzyme–carbamate inhibitor covalent tetrahedral intermediate; EI', the enzyme–carbamate inhibitor non-covalent complex; K_s , the dissociation constant of EI'.

inhibition constant (K_i), carbamylation rate constant (k_c), and bimolecular inhibition constant (k_i) for these 'pseudo-pseudo-substrate' inhibitions are calculated according to Eq. 1.⁷

Table 1. Kinetic data and correlation results for the pre-steady and steady states AChE inhibitions by alkane-1-*N*-butylcarbamate-*n*-ols (1–7)^{a,b}

Inhibitors	K_s (μM)	K_i (μM)	k_2 (10^{-3}s^{-1})	k_{-2} (10^{-3}s^{-1})	k_2/k_{-2}	k_c (10^{-3}s^{-1})
1	2.3 ± 0.4	1.5 ± 0.2	7.5 ± 0.4	5 ± 1	1.5 ± 0.3	3.1 ± 0.3
2	2.2 ± 0.2	1.4 ± 0.1	8.1 ± 0.8	5 ± 3	2 ± 1	3.5 ± 0.3
3	0.88 ± 0.09	0.36 ± 0.07	7.2 ± 0.2	3 ± 1	2.4 ± 0.8	3.6 ± 0.2
4	0.52 ± 0.05	0.20 ± 0.04	7.6 ± 0.1	3.1 ± 0.8	2.5 ± 0.6	3.9 ± 0.1
5	0.65 ± 0.03	0.3 ± 0.1	8.1 ± 0.5	4 ± 2	2 ± 1	4.1 ± 0.4
6	0.45 ± 0.04	0.20 ± 0.06	5.3 ± 0.7	4 ± 2	1.3 ± 0.7	4.6 ± 0.5
7	0.37 ± 0.03	0.13 ± 0.05	6.1 ± 0.3	3 ± 2	2 ± 1	4.9 ± 0.5
Correlations ^c	$-\log K_s$	$-\log K_i$	$\log k_2$	$-\log k_{-2}$	$\log(k_2/k_{-2})$	$\log k_c$
Slope	0.062 ± 0.009	0.08 ± 0.01	0.0019 ± 0.0006	0.012 ± 0.007	0.020 ± 0.006	0.08 ± 0.01
h	5.0 ± 0.2	5.0 ± 0.3	-2.13 ± 0.01	-2.2 ± 0.1	0.0 ± 0.1	-2.65 ± 0.02
R	0.950	0.968	0.800	0.612	0.792	0.986

^a Inhibitors 1–14 were synthesized from condensation of the corresponding 1,*n*-alkane-diol with 1.5 equiv of *n*-butyl isocyanate in presence of 1.5 equiv of NaH in tetrahydrofuran at 25 °C for 1 day to produce 1–7 (30–40% yield) and 8–14 (30–40% yield). All products were characterized by ¹H and ¹³C NMR spectra, high resolution mass spectra, and elemental analyses.

^b The enzyme inhibition reactions were determined by the Ellman assay²³ as described by Lin and co-workers^{6,22,24,25}. The K_i and k_c values were obtained from Eq. 1 by the Hosie's method.⁷ The K_s , k_2 , and k_{-2} values were obtained from Eq. 2 by the Lin's method.⁸ The *Electrophorus electricus* AChE (Sigma)-catalyzed hydrolysis of acetylthiocholine (0.1 mM) in the presence of 5,5'-dithio-bis-2-nitrobenzoate (0.1 mM) and inhibitors 1–7 were followed continuously at 410 nm on a UV–vis spectrometer (Agilent 8453) with or without a stopped-flow apparatus (Applied PhotoPhysics RX 2000).

^c Correlation of $-\log K_s$, $-\log K_i$, $\log k_2$, $\log k_{-2}$, $\log(k_2/k_{-2})$, and $\log k_c$ with the tether length (total backbone atoms) (*N*) (Fig. 2a).

Table 2. Kinetic data and correlation results for the pre-steady and steady states AChE inhibitions by 1,*n*-alkane-di-*N*-butylcarbamates (8–14)^{a,b}

Inhibitors	K_s (μM)	K_i (μM)	k_2 (10^{-3}s^{-1})	k_{-2} (10^{-3}s^{-1})	k_2/k_{-2}	k_c (10^{-3}s^{-1})
8	2.9 ± 0.2	0.36 ± 0.04	2.8 ± 0.1	0.35 ± 0.05	8 ± 1	3.0 ± 0.1
9	1.4 ± 0.1	0.25 ± 0.02	3.4 ± 0.1	0.62 ± 0.07	5.5 ± 0.5	3.3 ± 0.1
10	0.39 ± 0.02	0.15 ± 0.05	4.2 ± 0.2	1.6 ± 0.5	2.6 ± 0.9	4.0 ± 0.3
11	0.37 ± 0.04	0.16 ± 0.03	4.6 ± 0.2	2.0 ± 0.4	2.3 ± 0.5	4.1 ± 0.4
12	0.36 ± 0.02	0.16 ± 0.04	5.0 ± 0.3	2.2 ± 0.6	2.2 ± 0.6	4.6 ± 0.4
13	0.36 ± 0.02	0.16 ± 0.02	5.4 ± 0.2	2.4 ± 0.3	2.3 ± 0.3	4.9 ± 0.2
14	0.34 ± 0.02	0.17 ± 0.04	6.1 ± 0.3	3.1 ± 0.8	2.0 ± 0.5	5.3 ± 0.5
Correlations ^c	$-\log K_s$	$-\log K_i$	$\log k_2$	$-\log k_{-2}$	$\log(k_2/k_{-2})$	$\log k_c$
Slope	c.d. ^d	c.d.	0.024 ± 0.001	0.07 ± 0.01	1.5 ± 0.2	0.0180 ± 0.0009
h	c.d.	c.d.	-2.92 ± 0.03	-4.4 ± 0.3	-0.044 ± 0.009	-2.81 ± 0.02
R	c.d.	c.d.	0.994	0.939	0.914	0.994

^a Inhibitors 1–14 were synthesized from condensation of the corresponding 1,*n*-alkane-diol with 1.5 equiv of *n*-butyl isocyanate in presence of 1.5 equiv of NaH in tetrahydrofuran at 25 °C for 1 day to produce 1–7 (30–40% yield) and 8–14 (30–40% yield). All products were characterized by ¹H and ¹³C NMR spectra, high resolution mass spectra, and elemental analyses.

^b The enzyme inhibition reactions were determined by the Ellman assay²³ as described by Lin and co-workers^{6,22,24,25}. The K_i and k_c values were obtained from Eq. 1 by the Hosie's method.⁷ The K_s , k_2 , and k_{-2} values were obtained from Eq. 2 by the Lin's method.⁸ The *Electrophorus electricus* AChE (Sigma)-catalyzed hydrolysis of acetylthiocholine (0.1 mM) in the presence of 5,5'-dithio-bis-2-nitrobenzoate (0.1 mM) and inhibitors 1–7 were followed continuously at 410 nm on a UV–vis spectrometer (Agilent 8453) with or without a stopped-flow apparatus (Applied PhotoPhysics RX 2000).

^c Correlation of $-\log K_s$, $-\log K_i$, $\log k_2$, $\log k_{-2}$, $\log(k_2/k_{-2})$, and $\log k_c$ with *N*.

^d Discontinuity concave downwards (see Table 3).

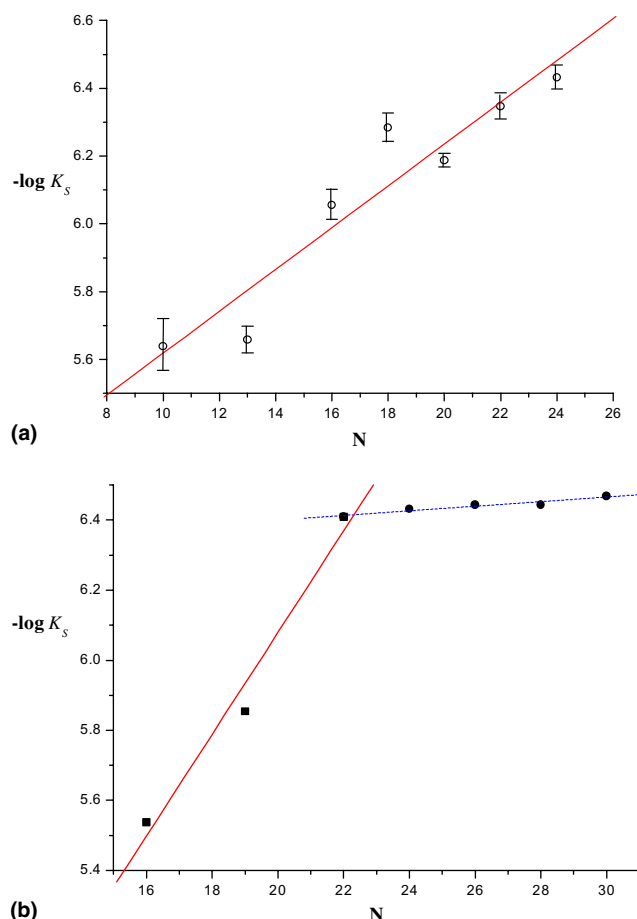


Figure 2. (a) Plot of the $-\log K_s$ values for the AChE inhibitions by tether inhibitors **1–7** against N . The standard error of the mean (SEM) is 0.0417 for this correlation ($n = 7$). The slope of 0.062 for this correlation (Table 1) indicates that these tether inhibitors are easy to pass through the hydrophobic, narrow gorge of the enzyme. (b) Plot of the $-\log K_s$ values for the AChE inhibitions by tether inhibitors **8–14** against N . A discontinuity of the $-\log K_s$ versus N plot, concave downwards, indicates a rate determining step change in the K_s step.^{10,12,13} The slope of 0.15 for short tether inhibitors **7–10** (solid line) is much higher than that for long tether inhibitors **10–14** (0.007) (dash line) because short tether inhibitors much depend on the hydrophobicity of the inhibitor to pass through the hydrophobic, narrow gorge of the enzyme^{16,17} (Fig. 3).

$$k_{app} = k_c[I]/(K_i(1 + [S]/K_m) + [I]) \quad (1)$$

Moreover, values of pre-steady state inhibition constant (K_s), k_2 , and k_{-2} (Scheme 2) for the pre-steady state inhibitions are calculated according to Eq. 2.⁸

$$k_{obs} = k_{-2} + (k_{-2}[I]/(K_s + [I])) \quad (2)$$

Alkane-1-*N*-butylcarbamate-*n*-ols (**1–7**) and 1,*n*-alkane-di-*N*-butylcarbamates (**8–14**) (Fig. 1) were characterized as ‘pseudo-pseudo-substrate’ inhibitors of AChE (Tables 1 and 2). The $-\log K_s$, $\log k_2$, $\log k_{-2}$, $-\log K_i$, $\log k_c$, and $\log k_i$ values for AChE inhibitions by inhibitors **1–7** (Table 1) and the $\log k_c$, $\log k_2$, and $\log k_{-2}$ values by inhibitors **8–14** (Table 2) were correlated with the Hansch hydrophobicity constant (π)⁹ or the tether length (N) (Fig. 2a) but not with σ^* and E_s against the Taft–Ingold¹⁰–Järv¹¹ equation (Eq. 3).

$$\log(k/k_0) = \rho^* \sigma^* + \delta E_s + \psi \pi \quad (3)$$

However, correlations of the $-\log K_s$, $-\log K_i$, and $\log k_i$ values against N (or π) for the AChE inhibitions by inhibitors **8–14** deviate from linearity (Tables 2 and 3). A discontinuity of the $-\log K_s$ versus N plot (Fig. 2b), concave downwards, is indicative of a rate determining step change.^{10,12,13} According to the Masson’s proposal,¹⁴ the pre-steady state K_s step is further divided into two steps, K_{s1} and K_{s2} , therefore, rate determining steps change in the pre-steady state K_s step in the AChE inhibition mechanisms by inhibitors **8–14** (Fig. 3). For long tether inhibitors **10–14**, the rate determining step is the K_{s1} step, which is formation of non-covalent pre-equilibrium protonated inhibitor^{6,15}–enzyme complex at the peripheral anionic site (PAS)^{14,16,21} that locates at the mouth of AChE, because long tether inhibitors are difficult to contact with the narrow mouth of the enzyme (PAS) (Fig. 3). However, for short tether inhibitors **8–10**, the rate determining step is the K_{s2} step, which is formation of non-covalent inhibitor–enzyme complex at the active site¹⁴ from the complex at PAS (Fig. 3). Thus, the slope of 0.15 in the $-\log K_s$ – N correlation for short tether inhibitors **7–10** is much higher than that for long tether inhibitors **10–14** (Fig. 2b and Table 3) because short tether inhibitors much depend on the hydrophobicity (N or π) of the inhibitor to pass through the hydrophobic, narrow gorge of the enzyme^{16,17} (Fig. 3).

Overall, the AChE inhibition mechanism by tether inhibitors **8–14** is proposed in Figure 3. The first step (K_{s1}) is formation of the non-covalent protonated inhibitor–enzyme PAS complex.¹⁴ The second step (K_{s2}) is formation of the non-covalent protonated inhibitor–enzyme active site complex.¹⁴ The third step (k_2) is formation of the covalent enzyme–inhibitor tetrahedral intermediate. The fourth step (k_c) is formation of carbamyl enzyme intermediate from the tetrahedral intermediate.

Table 3. Correlation results of discontinuities concave downwards for the $-\log K_s$ and $-\log K_i$ values of the AChE inhibitions by 1,*n*-alkane-di-*N*-butylcarbamates (**8–14**) against N

Correlations ^a	$-\log K_i$ $N \leq 22$	$-\log K_i$ $N \geq 22$	$-\log K_s$ $N \leq 22$	$-\log K_s$ $N \geq 22$
Slope	0.0063 ± 0.006	-0.005 ± 0.002	0.15 ± 0.02	0.007 ± 0.001
h	5.4 ± 0.1	6.94 ± 0.04	3.2 ± 0.4	6.29 ± 0.03
R	0.995	0.894	0.988	0.958

^a Correlation of the $-\log K_s$ and $-\log K_i$ values against N (Fig. 2b).

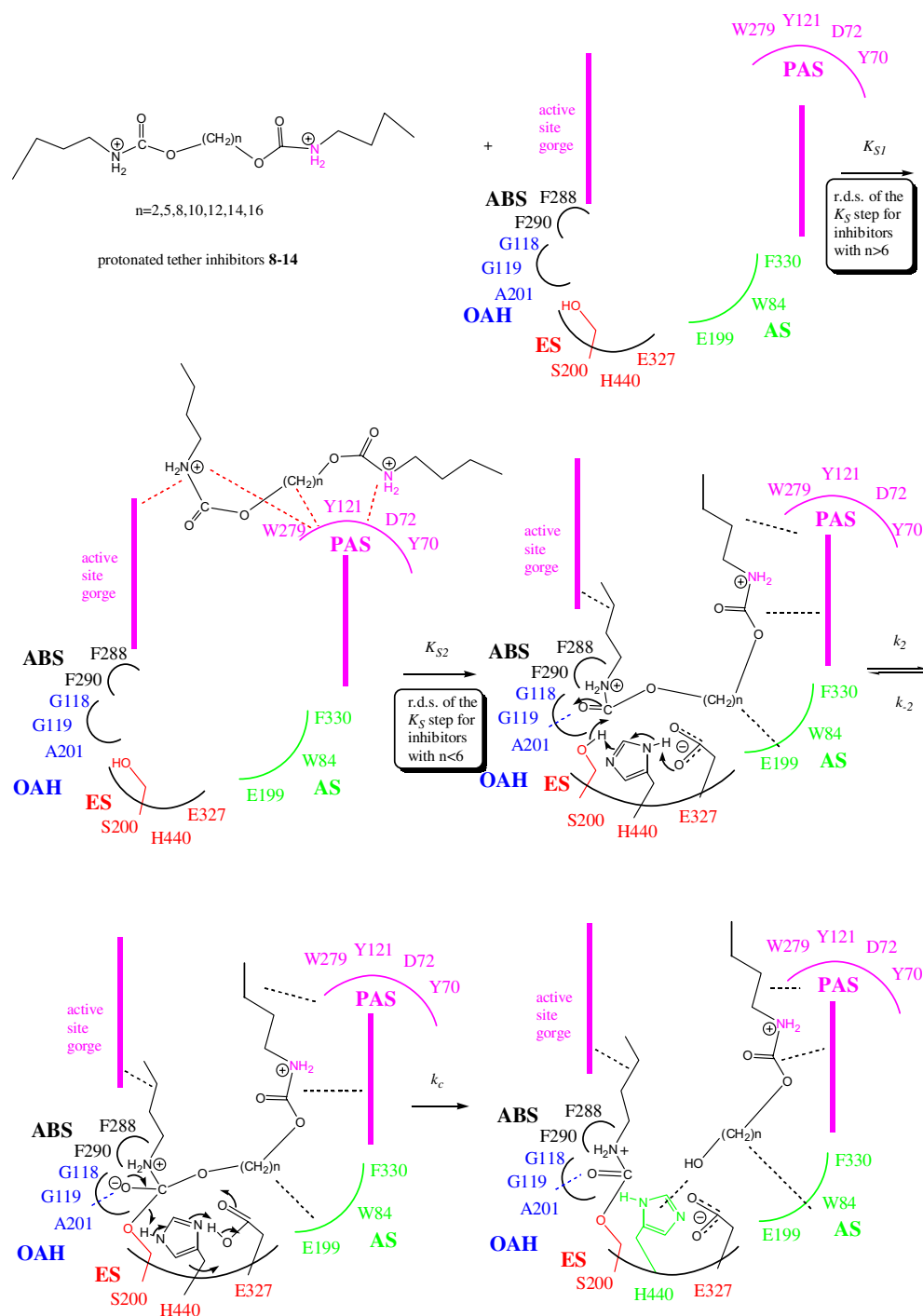


Figure 3. The proposed AChE inhibition mechanism by tether inhibitors **8-14**. Numbers refer to amino acid residue positions in *Torpedo californica* AChE.¹⁶ The active site of AChE contains of (a) an esteratic site (ES), (b) an oxyanion hole (OAH), (c) an anionic substrate binding site (AS), and (d) an acyl binding site (ABS). PAS is located at the entrance (mouth) of the active site gorge.¹⁶⁻²¹ The first step (K_{S1})¹⁴ is formation of the protonated inhibitor^{6,15}–enzyme PAS complex and is the rate determining step for long tether inhibitors **10-14**. The second step (K_{S2})¹⁴ is formation of the protonated inhibitor–enzyme active site complex and is the rate determining step for short tether inhibitors **8-10**. The third step (k_2) is formation of the inhibitor–enzyme covalent tetrahedral intermediate via the nucleophilic attack of active site S200. The fourth step (k_c) is formation of the carbamyl–enzyme intermediate from the tetrahedral intermediate.

Acknowledgements

We thank the National Science Council of Taiwan for financial support.

References and notes

1. Giacobini, E. In *Alzheimer's Disease: Molecular Biology to Therapy*; Becker, R., Giacobini, E., Eds.; Birkhauser: Boston, 1997; pp 187–204.

2. Soreq, H.; Zakut, H. *Human Cholinesterases and Anticholinesterases*; Academic: New York, 1993; pp 41–45.
3. Atack, J. R.; Yu, Q.-S.; Soncrant, T. T.; Brossi, A. *J. Pharmacol. Exp. Ther.* **1989**, 249, 194–202.
4. Geig, N. H.; Pei, X. F.; Soncrant, T. T.; Ingram, D. K.; Brossi, A. *Med. Res. Rev.* **1995**, 15, 3–31.
5. Bar-On, P.; Millard, C. B.; Harel, M.; Dvir, H.; Enz, A.; Sussman, J. L.; Silman, I. *Biochemistry* **2002**, 41, 3555–3564.
6. Lin, G.; Lai, C.-Y.; Liao, W.-C.; Liao, P.-S.; Chan, C.-H. *J. Chin. Chem. Soc.* **2003**, 50, 1259–1265.
7. Hosie, L.; Sutton, L. D.; Quinn, D. M. *J. Biol. Chem.* **1987**, 262, 260–264.
8. Lin, G.; Liao, W.-C.; Chiou, S.-Y. *Bioorg. Med. Chem.* **2000**, 8, 2601–2607.
9. Leo, A.; Hansch, C.; Elkins, D. *Chem. Rev.* **1971**, 71, 525–616.
10. Isaacs, N. *Physical Organic Chemistry*, 2nd ed.; Longman: UK, 1995; pp 163–165.
11. Järv, J.; Kesvatera, T.; Aaviksaar, A. *Eur. J. Biochem.* **1976**, 67, 315–322.
12. Hart, H.; Sedor, E. A. *J. Am. Chem. Soc.* **1967**, 89, 2342–2347.
13. Hoffmann, J.; Klicnar, J.; Sterba, V.; Vecera, M. *Collect. Czech. Chem. Commun.* **1970**, 35, 1387–1398.
14. Masson, P.; Xie, W.; Froment, M.-T.; Levitsky, V.; Fortier, P.-L.; Albaret, C.; Lockridge, O. *Biochim. Biophys. Acta* **1999**, 1433, 281–293.
15. Lin, G.; Lai, C.-Y.; Liao, W.-C.; Kuo, B.-H.; Lu, C.-P. *J. Chin. Chem. Soc.* **2000**, 47, 489–500.
16. Sussman, J. L.; Harel, M.; Frolow, F.; Oefner, C.; Goldman, A.; Toker, L.; Silman, I. *Science* **1991**, 253, 872–879.
17. Pleiss, J.; Fischer, M.; Schmid, R. D. *Chem. Phys. Lipids* **1998**, 93, 67–80.
18. Lin, G.; Tsai, H.-J.; Tsai, Y.-H. *Bioorg. Med. Chem. Lett.* **2003**, 13, 2887–2890.
19. Pang, Y.-P.; Quiram, P.; Jelacic, T.; Hong, F.; Brimijoin, S. *J. Biol. Chem.* **1996**, 271, 23646–23649.
20. Saxena, A.; Redman, A. M. G.; Jiang, X.; Lockridge, O.; Doctor, B. P. *Biochemistry* **1997**, 36, 14642–14651.
21. Savin, L.; Gaeta, A.; Fattorusso, C.; Catalanotti, B.; Campiani, G.; Chiasserini, L.; Pellerano, C.; Novellino, E.; McKissic, D.; Saxena, A. *J. Med. Chem.* **2003**, 46, 1–4.
22. Lin, G.; Chen, G.-H.; Ho, H.-C. *Bioorg. Med. Chem. Lett.* **1998**, 8, 2747–2750.
23. Ellman, C. L.; Courtney, K. D.; Andres, V., Jr.; Featherstone, R. M. *Biochem. Pharmacol.* **1961**, 7, 88–95.
24. Lin, G.; Tsai, Y.-C.; Liu, H.-C.; Liao, W.-C.; Cheng, C.-H. *Biochim. Biophys. Acta* **1998**, 1388, 161–174.
25. Lin, G.; Lai, C.-Y.; Liao, W.-C. *Bioorg. Med. Chem.* **1999**, 7, 2683–2689.